Repeatable ecological dynamics govern the response of experimental communities to antibiotic pulse perturbation

Cairns, Johannes

2020-10

Cairns , J , Jokela , R , Becks , L , Mustonen , V & Hiltunen , T 2020 , ' Repeatable ecological dynamics govern the response of experimental communities to antibiotic pulse þÿperturbation ' , Nature Ecology & Evolution , vol. 4 , no. 10 , pp. page

http://hdl.handle.net/10138/326255
https://doi.org/10.1038/s41559-020-1272-9

acceptedVersion

1. Extended Data

Figure #	Figure title One sentence only	Filename This should be the name the file is saved as when it is uploaded to our system. Please include the file extension. i.e.: *Smith_ED Fig1.jpg*	Figure Legend If you are citing a reference for the first time in these legends, please include all new references in the Online Methods References section, and carry on the numbering from the main References section of the paper.
Extended Data Fig. 1	Extended Data Fig. 1	Fig_S1.tiff	**Figure S1.** A t-SNE map showing *de novo* community clustering before, during and after recovery from antibiotic pulse at different antibiotic levels with or without immigration (N = 190). The different antibiotic levels are indicated by color coding, and the time points relative to the antibiotic pulse are indicated by different shapes. Low, intermediate and high antibiotic levels correspond to 4, 16 and 128 μg ml^{-1} streptomycin, respectively. All data points originate from the same t-SNE analysis and have been separated into two panels (with same arbitrary axis units) only for the sake of visual clarity of immigration effect (at high antibiotic level, post-recovery communities indicated by diamonds more often resume pre-disturbance composition in upper left-hand region).
Extended Data Fig. 2	Extended Data Fig. 2	Fig_S2.tiff	**Figure S2.** The extinction probability of species as a function of antibiotic level and the presence/absence of immigration (binomial glm estimate ± 95 % confidence intervals). Extinction is defined as the absence of a species after the antibiotic pulse (day 32 onwards) that was present prior to the pulse (day 16), and has been computed only for the species fulfilling these criteria in at least one experimental community (in total, 146 cases of

			extinction were observed). Low, intermediate and high antibiotic levels correspond to 4, 16 and 128 μg ml^{-1} streptomycin, respectively.
Extended Data Fig. 3	Extended Data Fig. 3	Fig_S3.tiff	**Figure S3.** Bacterial biomass estimated by optical density (OD) at 600 nm at different levels of antibiotic pulse (expressed in μg ml^{-1}) in the pre-disturbance (day 16), post-disturbance (day 32) and post-recovery (day 48) phases (mean ± standard deviation).
Extended Data Fig. 4	Extended Data Fig. 4	Fig_S4.tiff	**Figure S4.** Global comparative view of community composition as shown by Kullback-Leibler (KL) divergence across all samples (N = 190). The color scale from blue to red indicates the degree to which community composition differs between two communities. KL divergence has been computed from species compositional data. The heat map has been color-annotated for the different immigration and antibiotic treatments and experimental phases. Low, intermediate and high antibiotic levels correspond to 4, 16 and 128 μg ml^{-1} streptomycin, respectively.
Extended Data Fig. 5	Extended Data Fig. 5	Fig_S5.tiff	**Figure S5.** Competitive fitness landscapes across all samples during the antibiotic pulse and recovery phases (N = 126). The color scale from blue to red indicates the degree to which the competitive fitness landscapes are correlated between two communities. Correlations have been computed from competitive fitness data for each species in the communities. The heat map has been color-annotated for the different immigration and antibiotic treatments and experimental phases. Low, intermediate and high antibiotic levels correspond to 4, 16 and 128 μg ml^{-1} streptomycin, respectively. The black boxes show the data presented at species-level detail in Figure 4 in the main text.
Extended Data Fig. 6	Extended Data Fig. 6	Fig_S6.tiff	**Figure S6.** Correlation of competitive fitness landscapes

			within replicates in each experimental treatment (mean + 95 % confidence interval). Correlations have been computed from competitive fitness data for each species in the communities. The figure aggregates the pairwise correlation values shown for each replicate pair within treatments in Figure S4. Low, intermediate and high antibiotic levels correspond to 4, 16 and 128 μg ml^{-1} streptomycin, respectively.
Extended Data Fig. 7	Extended Data Fig. 7	Fig_S7.tiff	**Figure S7.** Percentage of variance in the competitive fitness of species explained by the experimental treatments (antibiotic level and presence / absence of species immigration) and species traits (antibiotic MIC and intrinsic growth rate). The variance partitioning is based on ANOVA on competitive fitness performed separately for the antibiotic pulse and recovery phases (detailed results are presented in Tables S1 and S2).
Extended Data Fig. 8	Extended Data Fig. 8	Fig_S8.tiff	**Figure S8.** Illumina read recruitment (median per species) in whole genome alignments for deep sequencing data (two upper panels) or raw 16S rRNA amplicon data (bottom panel). The HAMBI codes of the species are indicated in the horizontal axis, with two exceptions: K12 and RP4 denote the chromosome and plasmid sequence, respectively, from *E. coli* JE2571. Read recruitment in whole genome alignments is indicated as number of reads (100 bp) in 1,000 bp blocks, and needs to be divided by 10 ((100 bp × read count)/(1,000 bp block)) to obtain an estimate of genome coverage. For instance, a median read count of 1,000 corresponds to roughly 100× genome coverage. In the uppermost panel, deep sequencing data was mapped separately to the genome of each individual species, and in the middle panel, the data was mapped to a multi-FASTA file containing all the genomes, producing comparable results. 16S rRNA amplicon read

			counts have been normalized to 15,000 reads per sample.
Extended Data Fig. 9	Extended Data Fig. 9	Fig_S9.tiff	**Figure S9.** Deep sequencing read recruitment across the genomes of abundant species. Genomic position is indicated as relative position (0–1) across the whole chromosome for closed genomes or largest contig for draft genomes. Read recruitment in whole genome alignments is indicated as number of reads (100 bp) in 1,000 bp blocks, and needs to be divided by 10 ((100 bp × read count)/(1,000 bp block)) to obtain an estimate of genome coverage.

2. Supplementary Information:

A. Flat Files

Item	Present?	Filename This should be the name the file is saved as when it is uploaded to our system, and should include the file extension. The extension must be .pdf	A brief, numerical description of file contents. i.e.: *Supplementary Figures 1-4, Supplementary Discussion, and Supplementary Tables 1-4.*
Supplementary Information	Yes	SI.pdf	Supplementary Tables S1 to S2
Reporting Summary	Yes	nr-reporting-summary.pdf	
Peer Review Information	Yes	PRFile_Cairns.pdf	

Repeatable ecological dynamics govern the response of experimental communities to antibiotic pulse perturbation

Johannes Cairns[1,2,3*†], Roosa Jokela[3,4*], Lutz Becks[5,6], Ville Mustonen[2,7], Teppo Hiltunen[3,8†]

ORCIDs: JC: 0000-0003-1329-2025; RJ: 0000-0002-4144-6573; LB: 0000-0002-3885-5253; VM: 0000-0002-7270-1792; TH: 0000-0001-7206-2399

[1]Wellcome Sanger Institute, Cambridge, CB10 1SA, UK

[2]Organismal and Evolutionary Biology Research Programme (OEB), Department of Computer Science, 00014 University of Helsinki, Finland

[3]Department of Microbiology, P.O. Box 56, 00014 University of Helsinki, Finland

[4]Human Microbiome Research Program (HUMI), Faculty of Medicine, University of Helsinki, P.O. Box 21, Haartmaninkatu 3, 00290 Helsinki, Finland

[5]Max Planck Institute for Evolutionary Biology, Department of Evolutionary Ecology, Community Dynamics Group, August Thienemann Str. 2, 24306 Plön, Germany

[6]Limnological Institute University Konstanz, Aquatic Ecology and Evolution, Konstanz, Germany

[7]Helsinki Institute for Information Technology, Institute of Biotechnology, University of Helsinki, Finland

[8]Department of Biology, 20014 University of Turku, Turku, Finland

[*]These authors contributed equally to this work

[†]Co-corresponding authors: Johannes Cairns (e-mail: johannes.cairns@helsinki.fi) and Teppo Hiltunen (e-mail: teppo.hiltunen@utu.fi)

Abstract

In an era of pervasive anthropogenic ecological disturbances, there is a pressing need to understand the factors constituting community response and resilience. A detailed understanding of disturbance response needs to go beyond associations and incorporate features of disturbances, species traits, rapid evolution and dispersal. Multispecies microbial communities experiencing antibiotic perturbation represent a key system with important medical dimensions. However, previous microbiome studies on the theme have relied on high-throughput sequencing data from uncultured species without the ability to explicitly account for the role of species traits and immigration. Here we serially passaged a 34-species defined bacterial community through different levels of pulse antibiotic disturbance, manipulating the presence or absence of species immigration. To understand the ecological community response measured by amplicon sequencing, we combined initial trait data measured for each species separately and metagenome sequencing data revealing adaptive mutations during the experiment. We found that the ecological community response was highly repeatable within the experimental treatments, which could be partly attributed to key species traits (antibiotic susceptibility and growth rate). Increasing antibiotic levels were also coupled with increasing species extinction probability, making species immigration critical for community resilience. Moreover, we could detect signals of antibiotic resistance evolution occurring within species at the same time scale, leaving evolutionary changes in communities despite recovery at the species compositional level. Together these observations reveal a disturbance response which appears as classic species sorting but is nevertheless accompanied by rapid within-species evolution.

Introduction

In the Anthropocene[1] characterized by anthropogenic perturbations of environments ranging in scale from the individual organism (e.g. gut microbiota of mammal) to the global ecosystem (e.g. climate change and loss of biodiversity), it is paramount to understand factors determining biological resilience[2]. Understanding how the effects of perturbations percolate through the ecosystem is vital to better understand the risks and benefits of human driven control efforts in the restoration and conservation of populations. For instance, antibiotic treatment affects not only the pathogen population but also off-target species in the microbiota of the patient, promoting the spread of antimicrobial resistance[3]. Rational interventions require a detailed, ideally mechanistic, understanding that goes beyond associations, integrating community dynamics, species traits, environmental variables, evolutionary events and stochasticity. However, we are far from such an understanding, which has in part been attributed to the sparsity of controlled studies amidst *in vivo*, field and theoretical studies[4]. Nevertheless, recent advances in predictive modeling suggest that such an understanding is possible for certain rapidly evolving systems[5].

A notable case of interest is the response of multispecies bacterial communities to perturbations by antibiotics, pharmaceuticals and other compounds of an anthropogenic origin. Understanding this response can be critical, among others, for rational therapeutics to mitigate unwanted effects on patient health caused by changes in the gut microbiota (e.g. *Clostridioides difficile* infection[6]), management of waste water treatment to ensure the maintenance of key functionalities in bacterially driven processes[7], and redesigning of agricultural practices to maintain microbiota contributing to crop health and productivity[8].

Traditionally, ecological timescales have been considered shorter than evolutionary timescales, causing ecological processes to drive the community response to environmental change. The community response to perturbation is therefore expected to be determined by selection on pre-existing traits at the species level[9]. Selection may also act on the standing genetic variation within populations and affect the community response to perturbation[10-13]. However, the role of standing trait variation at the species level in the bacterial disturbance response remains unclear, because large population sizes and short generation times can render bacterial populations virtually unlimited by mutation supply. This leads to the omnipresence and rapid generation of intraspecific trait variation, which can play a major role in ecological dynamics[14], especially since mutations in the bacterial genome can have strong effects on traits. For instance, a single point mutation in the gene *rpsL* can make a bacterium over 250-fold more resistant to the antibiotic streptomycin[15]. Overall, strong evidence has emerged in recent decades showing that rapid evolution can alter ecological dynamics in communities across a range of systems, even those with lower rates of evolution compared to microbial systems[16]. Similarly, a community ecology context can be important for evolutionary trajectories[17]. While there is an extensive number of studies on both the species compositional effects of antibiotic perturbation on the microbiome and the genetics of antibiotic resistance evolution in individual species, both aspects have rarely been analyzed together. Furthermore, high-throughput sequencing based approaches allowing the investigation of mutations in longitudinal microbiome data have focused on *in vivo* and field samples where the species are uncultured and the pre-existing traits of the species cannot be explicitly estimated[18]. This may hinder the ability to assess the importance of evolution relative to species sorting in the perturbation response of communities.

Ecological resilience describes the ability of a community not only to withstand a perturbation (ecological resistance) but also to recover from it. Studies have shown variable results concerning the resilience of the human gut microbiota to antibiotic perturbations at high, clinical concentrations[19-21].

Effects of antibiotics that may or may not completely reverse after the perturbation include reduced community stability[22] and diversity[23], which have been associated with adverse health consequences in patients[24,25]. However, the sparsity of longitudinal studies and the variability in time points sampled since the perturbation pose challenges for comparing studies and assessing whether the communities are still in a state of recovery at the time of sampling. Moreover, the conditions determining a particular community response remain unclear. These include factors such as the level of perturbation and species immigration[26], a key feature of microbial communities and form of bacteriotherapy (e.g. probiotic supplementation after antibiotic treatment)[27]. There is also a practical need to understand how the disturbance and immigration responses of bacterial communities interact. For example, this information is critical for the design of minimal artificial communities to replace fecal microbiota transplantation (FMT), where gut microbial communities disturbed by antibiotic pulses are treated by a fecal "immigration" to restore a healthy microbiota[28].

Here we used a 34-species model bacterial community to examine the role of ecological and evolutionary processes in the community response to different levels of pulse disturbance by the aminoglycoside antibiotic streptomycin in the absence or presence of species immigration. We performed a serial passage experiment, collecting amplicon data to track ecological dynamics and deep sequencing data to track evolutionary dynamics, and combined experimental data with pre-existing trait data on community members (Figure 1). We found that communities responded sensitively and repeatably to the different environments. This could be linked to species sorting and selection on their traits (growth rate and antibiotic susceptibility) as well as an increase in the extinction probability of particular species at increasing antibiotic levels in the absence of immigration. Adaptive mutations also occurred but could not be linked to the ecological dynamics. Despite the sensitive response to the perturbation, communities were able to recover close to the initial community state in all but the highest antibiotic level. However, the loss of species as a function of antibiotic level as

well as the occurrence of evolutionary changes within species still left persistent changes in communities, compromising their resilience over the long term. Importantly, immigration played a key role in resilience at the species level by preventing species extinctions.

Results

Both antibiotic level and immigration strongly determine ecological resilience

The communities were compositionally sensitive to the different antibiotic levels and the presence of immigration (Figures 2 & 3; Extended Data Figure 1). Machine learning models could be trained to correctly predict the antibiotic level during the antibiotic pulse from species composition data (random forest, rf, model using community composition data from all treatments immediately post-perturbation to classify antibiotic level: permutation test $p < 0.001$, accuracy estimated by leave-one-out cross-validation, LOOCV, 0.88). However, the ability to distinguish between the antibiotic levels decreased after the recovery period (rf model using community composition data from all treatments immediately post-perturbation to classify antibiotic level: permutation test $p < 0.001$, LOOCV accuracy 0.53). In contrast, machine learning models could correctly classify the immigration treatment only after the recovery period (rf model using community composition data from all treatments immediately post-perturbation to classify immigration presence/absence: permutation test $p = 0.19$, LOOCV accuracy 0.53; rf model for immigration post-recovery: permutation test $p < 0.001$, LOOCV accuracy 0.69). These results suggest that the antibiotic perturbation had a compositional effect specific to the antibiotic level, this effect decreased with recovery, and the latter process was influenced by species immigration.

To further investigate factors determining ecological resilience, we inspected the effect of the disturbance on two measures of entropy. We used the Shannon diversity (information entropy incorporating species richness and evenness) after the disturbance and Kullback-Leibler (KL) divergence (relative entropy comparing species composition) in individual communities over time after the disturbance relative to the pre-disturbance state[29] (Figure 3). An analysis of this data shows that diversity decreased (ANOVA for linear regression model on Shannon diversity with lowest AIC value; antibiotic $F_{3,60} = 12.1$, $p < 0.001$; the immigration treatment did not have a significant effect during the antibiotic pulse and was not included in the best model; Figure 3a) and community composition became increasingly altered as a function of antibiotic level during the pulse, and that immigration enhanced community recovery after the pulse (ANOVA for gls model on KL divergence with lowest AIC value: antibiotic level $F_{3,118} = 19.8$, $p < 0.001$; immigration $F_{1,118} = 6.33$, $p = 0.013$; recovery time $F_{1,118} = 8.31$, $p = 0.005$). Pairwise comparisons of estimated marginal means for KL divergence show significant differences ($p < 0.02$) between all of the antibiotic levels except for the control and lowest level.

Persistent alterations in community composition were only observed for the highest antibiotic level in the absence of immigration (Figure 3b). Increasing antibiotic levels increased, however, species extinction probability, which was strongly counteracted by immigration (ANOVA for binomial glm model with lowest AIC value: antibiotic $\chi^2_{3,1643} = 22.3$, $p < 0.001$; immigration $\chi^2_{1,1646} = 27.3$, $p < 0.001$; species $\chi^2_{25,1618} = 166$, $p < 0.001$; antibiotic × immigration $\chi^2_{2,1615} = 7.52$, $p = 0.057$; Extended Data Figure 2). Therefore, in the absence of immigration, loss of species caused alterations in community composition, and the magnitude of the effect was proportional to the magnitude of the perturbation. The reported community effects of antibiotic level and immigration are unlikely to have been affected by changes in total bacterial biomass, since similar levels of biomass were observed across the experimental conditions and time points (Extended Data Figure 3). This indicates

that the relative abundance of species is here a close approximation of absolute abundance, which is not always the case in microbial community studies and can have important implications for study conclusions[30].

Ecological dynamics are highly repeatable within antibiotic and immigration treatments

We next investigated whether increasing antibiotic levels are coupled with decreased repeatability[22] in community trajectories, as this could be a signal of alternative stable states (including bi- and multi-stability), stochastic species extinctions or adaptive *de novo* mutations. In contrast with this expectation, we found relatively low levels of divergence in community states within each antibiotic and immigration treatment (Extended Data Figure 4). To further examine this result, we estimated the competitive fitness of each species in the community during the antibiotic pulse or recovery phase using the replicator equation from evolutionary game theory. In this approach, the frequency change of one species over time is considered to be an outcome of its fitness reduced by the average fitness of the community. We found that the competitive fitness of the species responded repeatably to the different antibiotic levels, and that many of the species displaying a strong positive response during the pulse displayed an inverse response during the recovery phase (intermediate antibiotic level without immigration illustrated in Figure 4; for complete data for all treatments, see Extended Data Figures 5 and 6). We also found that increasing antibiotic levels increased fitness variance (particular species exhibited very high or low competitive fitness values), as hypothesized previously[31], which is reflected by increasingly correlated competitive fitness landscapes during the antibiotic pulse and becomes reversed during the recovery phase (Extended Data Figures 5 and 6). We could attribute 10–13 % variation in the competitive fitness of species during the antibiotic pulse and recovery phases to the interplay between antibiotic level and key species traits, intrinsic

antibiotic susceptibility (streptomycin MIC) and intrinsic growth rate (r_{max}; Tables S1 and S2; Extended Data Figure 7). For instance, two species with high growth rate combined with high antibiotic susceptibility, *Aeromonas caviae* HAMBI 1972 (MIC = 0.75 μg ml^{-1}) and *Pseudomonas chlororaphis* HAMBI 1977 (MIC = 8.0 μg ml^{-1}), decreased in abundance and competitive fitness at increasing antibiotic levels (Figures 2 and 4). Potential reasons for why a higher proportion of variation in competitive fitness could not be explained by species traits despite the highly consistent ecological response include the presence of important unmeasured species traits, species interactions, or non-linear system-level behavior (e.g. dramatic community change only after particular concentration reached). Such information would be useful for predictive modelling.

To more precisely inspect the low levels of community divergence observed within treatments (Extended Data Figure 4), we quantified the repeatability of community trajectories within each antibiotic and immigration treatment using the diversity dissimilarity index[33] which relates diversity pooled over replicate communities to the mean diversity of replicate communities. This yields a value between zero and one, where zero indicates that replicate communities are identical and one that they are completely different. The community trajectories were highly repeatable (close to zero) in the different experimental treatments when species were weighted based on their abundance, although a slight (approximately 5 %) decay in repeatability was observed for the highest antibiotic level during the pulse (Shannon entropy panel in Figure 5). The high repeatability suggests that rare stochastic mutational events are unlikely to have been a major driver of the ecological dynamics of the abundant species. However, there was a higher decay in repeatability when species were given equal weight regardless of abundance, indicating that low-abundance species account for most of the loss in repeatability (species richness panel in Figure 5). When combined with the finding that the extinction probability of species increased as a function of antibiotic level (Extended Data Figure 2), these results suggest that the stochasticity introduced by antibiotic perturbation was at least

partially accounted for by low-abundance species being driven extinct differentially between replicate communities. Nevertheless, a potential role for evolutionary rescue in the stochasticity of the ecological dynamics of low-abundance species cannot be ruled out.

Antibiotic resistance mutations occur despite repeatable ecological dynamics

To investigate mutational dynamics, we deep-sequenced three of the eight replicate communities during and after recovery from the antibiotic pulse. From these community metagenomes, we could extract whole-genome data for abundant species with sufficient genome coverage in a particular community. We focused on genes estimated to be under selection (N = 91) based on containing more nonsynonymous hits in independent populations than expected by chance. Most of these genes contained mutations across experimental treatments, suggesting that they represent adaptations to the general experimental conditions rather than treatment-specific adaptations (Figure 6). Nevertheless, antibiotic and immigration also significantly enriched mutations for a small subset of genes even when controlling for the presence or absence of whole-genome data (and thereby, information for a particular mutational target) for the different species in each community metagenome (PERMANOVA for binary vectors of mutated genes, i.e. mutational profiles: species R^2 = 0.81, $p < 0.001$; antibiotic $R^2 = 0.015$, $p < 0.001$; immigration $R^2 = 0.0082$, $p < 0.001$).

Among the mutational targets that occurred only in the presence of the antibiotic, several have been previously associated with increased levels of streptomycin or aminoglycoside resistance or with the presence of these agents, suggesting that antibiotic-related adaptations occurred during the experiment. These genes include *rpsL* (encoding ribosomal protein S12, a common streptomycin resistance target)[34], *rsmG* (ribosomal methyltransferase)[35], *phoQ* (PhoP-PhoQ two-component regulatory system)[36], *cya* (adenylate cyclase)[37], *cra* (catabolite repressor/activator)[37], *cspA* (cold shock

252 protein)[38], *relA* (GTP pyrophosphokinase mediating stringent response)[15] and *spoT* ((p)ppGpp syn-
253 thase/hydrolase mediating stringent response)[15]. Most of these mutations occurred in the intermedi-
254 ate or highest antibiotic concentration, while displaying no general pattern with respect to the pres-
255 ence or absence of immigration (observed only without immigration: *rpsL* (1×) and *cspA* (2×); only
256 with immigration: *rsmG* (2×); both without and with immigration: *cra* (2×), *cya* (13×), *phoQ* (2×),
257 *relA* (4×); Figure 6). Notably, mutations in a particular gene were not required for a species to suc-
258 ceed at a given antibiotic level. For instance, an *rpsL* mutation in *Agrobacterium tumefaciens*
259 HAMBI 105 and *rsmG* mutations in *Pseudomonas chlororaphis* HAMBI 1977 only occurred in a
260 subset of the replicates where the species displayed high abundance in the respective antibiotic
261 treatment (Figure 6). The low level of within-treatment repeatability in mutational targets contrasts
262 with the high level of within-treatment repeatability in ecological trajectories for abundant species.
263 Therefore, we could not detect an influence of genomic evolution on the ecological dynamics with
264 the methods employed in this study, although we acknowledge the limitations of our approach (fo-
265 cusing on abundant species in a subset of replicates).
266
267 **Discussion**
268
269 Using a controlled setup to investigate the antibiotic response of a multispecies bacterial community
270 in the presence and absence of species immigration, we found that the replicate communities re-
271 sponded repeatably to the different treatments, with the magnitude of the community response and
272 persistent community changes increasing with increasing antibiotic levels. The community effects
273 of antibiotics expectedly included both abundance changes and extinctions of particular species.
274 Persistent community changes were linked to increasing species extinctions at increasing antibiotic
275 level, which prevented abundant high-growth-rate species sensitive to the antibiotic from rebound-
276 ing to their pre-disturbance abundance during the recovery phase, and could be counteracted by

277 species immigration. This was not a straightforward outcome, since the original community compo-
278 sition may not have recovered despite reintroduction of sensitive species if communities had
279 reached an alternative stable state during the antibiotic pulse. Overall, these findings highlight the
280 importance of classic and relatively simple ecological processes, species sorting and immigration,
281 in defining how microbial communities respond to antibiotic perturbation.
282
283 The high level of repeatability of the ecological dynamics in our study appears to contrast with pre-
284 vious studies showing decreased stability[22] and bistability[39] in microbial communities following
285 antibiotic exposure. However, similar to these studies, the minor decay in repeatability we observed
286 did occur under high antibiotic levels (Figure 5). Furthermore, at the intermediate antibiotic level,
287 certain replicate communities experienced a more dramatic decline in diversity compared to others
288 (Figure 3a and Extended Data Figure 1), indicating that this antibiotic level may be close to a tip-
289 ping point concentration where bistable system-level behavior is possible. Quantifying these effects
290 more precisely would have required experimenting with a wider range of antibiotic concentrations.
291 Moreover, a previous study shows that high rates of immigration can fuel adaptation to antibiotics
292 by increasing the supply of genetic variation[40]. Therefore, higher levels of immigration could poten-
293 tially have exacerbated the role of evolution in our immigration treatment such that replicate com-
294 munities would have diverged more during the antibiotic pulse, as species containing adaptive mu-
295 tations by chance or the timing of occurrence of these mutations would differ between them. This
296 could also have decreased the rate of recovery in the immigration treatment, since there would have
297 been an increased likelihood of communities reaching alternative stable states and larger differences
298 in post-disturbance genetic composition may have slowed down species compositional recovery
299 rate. However, establishing this would have required experimenting with different levels of immi-
300 gration. Therefore, the level of ecological repeatability observed may be influenced by a number of
301 study conditions.

We also found adaptive mutations sweeping to high frequencies in populations of individual species, although we could not connect these with species abundance. This shows that the disturbance response in microbial systems results from a combination of ecological and evolutionary processes operating at the same timescale. However, connecting these processes may not always be straightforward[41.] Similar to our finding, in a recent analysis of longitudinal linked-read sequencing data from human gut microbiota subjected to antibiotic treatment, antibiotic resistance mutations were found to sweep to high frequencies in the populations of single species without necessarily resulting in an increased abundance of the species in the community[18]. In a microbial community, species sorting and adaptive mutations occur simultaneously in multiple species, and all these factors have the potential to interact, making it challenging to disentangle ecological from evolutionary processes. Furthermore, in a number of conditions, relative fitness increases within a species based on allele frequency changes do not translate into changes in absolute fitness (population size)[32]. In a multispecies setup, the competitive release of an adapted species may be suppressed, for example, by the presence of other abundant species with relatively low intrinsic antibiotic susceptibility and equal or higher resource use ability. The occurrence of a fitness trade-off between growth rate and antibiotic resistance[42] could also make the net fitness advantage of antibiotic resistance low, causing a weak ecological effect difficult to detect in a multispecies setup. Importantly, whatever the underlying mechanism, this study supports the notion that within-species adaptive evolution can occur during a perturbation even when this is not readily suggested by the ecological dynamics.

Our findings have important implications for the understanding and management of ecological resilience. Although we found similar outcomes from antibiotic perturbation as those reported in human gut microbiome studies, such as decreased diversity[23], these outcomes were mostly limited to the community state at the end of the perturbation, and were followed by community recovery close

to the pre-disturbance state. This is non-trivial taken that priority effects[43] or the presence of alternative stable states[44,45] could cause a perturbed community to recover to an altered state, and emphasizes the need to assess ecological resistance during perturbations separately from recovery and longer-term resilience[46]. More generally, since the advent of amplicon and metagenomic sequencing, changes in bacterial communities have been found in response to a plethora of environmental factors, but our findings suggest that such changes may not persist and a need for caution in data interpretation in the absence of longitudinal data. Nevertheless, despite the communities mostly rebounding, species extinctions, which were more likely at increasing antibiotic levels, left persistent marks in community composition, similar to recent findings from human gut microbiota[20], although species immigration enabled community recovery. This indicates that storing and reintroducing susceptible low-abundance species with key functionalities could play a crucial role in human management of ecological disturbances. Ecological resilience was most notably compromised for the highest antibiotic level, suggesting that in a therapeutic context, intermediate antibiotic levels may represent a desirable compromise minimizing off-target effects assuming they are sufficient to treat a pathogen[3]. Notably, here we considered only a single pulse disturbance, while communities often face multiple disturbances, with historical disturbance regimes frequently priming populations, communities and ecosystems, both ecologically and evolutionarily, to similar disturbances in the future[39,47,48]. Therefore, the types of persistent ecological (lost species) and evolutionary (resistance mutations) changes observed in this study may have important consequences for the response of communities to future perturbations.

Methods

Strains and culture conditions

The liquid medium used in the experiment was specifically developed for complex communities and a long culture cycle. An artificial bacterial community consisting of 34 species (for species list, see Supplementary Materials in [49]) was almost entirely chosen from the HAMBI Culture Collection, University of Helsinki, except for *Escherichia coli* K-12 strain JE2571[50]. The bacteria are gram-negative and represent three classes (Alpha-, Beta- and Gammaproteobacteria) in the phylum Proteobacteria and three classes (Chitinophagia, Flavobacteriia and Sphingobacteriia) in the phylum Bacteroidetes. The species are not representative of a particular natural system but were rather selected based on growth in simple, uniform laboratory conditions. Different versions of the artificial community have been used in two previous studies[49,51], where details are reported regarding its construction and the phenotypic and genomic characteristics of the species.

A medium was specifically refined for the selected community and long culture cycles. The co-culture medium contains 1 g l^{-1} R2A broth (Labema, Helsinki, Finland) and 0.5 g l^{-1} of cereal grass medium (Ward's Science, St Catharines, ON, Canada) in M9 salt solution. The cereal grass medium stock was prepared by autoclaving it in deionized H_2O and filtering through 5 µl to remove particulate matter.

Serial passage experiment

A 48-day serial passage antibiotic pulse experiment was performed consisting of three epochs: 16 days without streptomycin to allow the community composition to acclimatize to experimental conditions, 16 days with streptomycin at the concentrations 4, 16, and 128 µg ml^{-1}, and 16 days without antibiotics to allow the community to recover (Figure 1). The experiment included an antibiotic-free control treatment. The experiment was performed in a full-factorial design without and with immi-

gration consisting of adding an inoculum of the original community at each transfer. Each treatment combination was replicated eight times.

The experiment was conducted in ABgene™ 96 Well 2.2 ml Polypropylene Deepwell Storage Plates (Thermo Fisher Scientific, Waltham, MA, USA) in the co-culture medium. Prior to starting the experiment, all the strains were transferred to the co-culture medium and cultured for 96 hours at 28 °C / 50 rpm. Following this, they were pooled together in equal volumes and freeze-stored with 30% glycerol at –80 °C. To start the experiment, 10 µl of 100-fold diluted freezer-stock community was added to each well containing 500 µl of medium and 50 µl of sterile dH_2O to compensate the dilution caused by streptomycin additions. Equal volumes were used instead of using more precise methods such as plate counting or flow cytometry to equalize cell numbers for each species prior to starting the experiment since we assumed that uncertainty in the latter methods and differences between species in cell viability and revival from frozen inoculum would nevertheless have introduced substantial initial differences in species abundances. We therefore accepted that the starting conditions are biased toward high growth ability species which would in any case have been likely to rise to dominance rapidly during the initial culture cycles (first 16-day acclimation epoch). Culturing throughout the experiment was performed at 28 °C / 50 rpm. The experiment was maintained every 96 hours by transferring 50 µl, about 10%, to fresh medium prepared as in the beginning of the experiment (representing approx. 3.33 bacterial generations per culture cycle with the minimal assumption that bacteria multiply until reaching carrying capacity). For the immigration treatment, 10 µl of 100-fold diluted freeze-stored community was also added. For cultures containing streptomycin, the dH_2O was replaced with an equal volume of the appropriate streptomycin stock solution.

Data collection

The pre-existing phenotypic trait data for community members used in this study, including intrinsic growth rate and streptomycin minimum inhibitory concentration (MIC) values, was obtained as described previously[49]. To monitor bacterial density during the serial passage experiment, optical density values at 600 nm wavelength (OD_{600nm}) were measured from old cultures prior to the disturbance (day 16), after the disturbance (day 32), and after the recovery period (day 48) using a well plate reader (Tecan Infinite M200 well-plate reader, Tecan Trading AG, Switzerland). Samples from time points 16 days (before streptomycin addition), 32 days (last time point with streptomycin) and 48 (final time point) days were also frozen in glycerol at –80 °C for further analysis.

DNA was extracted from the original freezer-stock community and the first three (1–3) out of eight experimental replicate communities from days 16, 32 and 48 in the serial passage experiment for a first batch of amplicon sequencing and the deep sequencing. A second batch of DNA extraction and amplicon sequencing was later performed for the remaining five replicates (4–8). DNA extraction was performed directly on freeze-stored samples without regrowing with the DNeasy 96 Blood & Tissue Kit (Qiagen, Hilden, Germany) according to the manufacturer's instructions using 400–600 µl of defrosted sample. DNA concentrations were measured with the Qubit™ 2.0 (Life Technologies Corporation, Carlsbad, CA, USA) fluorometer using the Qubit™ dsDNA HS Assay Kit (Thermo Fisher Scientific, Waltham, MA, USA). Paired-end 16S rRNA amplicon sequencing (V3 and V4 regions, 2 × 300 bp; all three time points) and metagenomic deep sequencing (2 × 101 bp; only days 32 and 48) was performed by the Institute for Molecular Medicine Finland (FIMM) using the Illumina MiSeq and Illumina HiSeq2500 platforms, respectively, employing in-house protocols similar to those described before[49].

Sequence data processing

For 16S rRNA amplicon data, raw reads were first paired using the paired-end read merger Pear v0.9.6[52] with defaults settings. Adapters and primers were removed from the paired reads using Cutadapt v1.10[53] with the options -q 28 (quality-cutoff for trimming 3′ end of read), -n 2 (two rounds of adapter searching), -e 0.2 (maximum error rate of 20 % for adapter identification), and --minimum-length 400 (discarding reads < 400 bp after quality control steps). Read quality was controlled with FastQC v0.11.8 (www.bioinformatics.babraham.ac.uk/projects/fastqc) and MultiQC v1.7[54] before and after running Pear and Cutadapt. USEARCH v1.10[55] was used to quality filter the reads using the --fastq-filter command with the options -fastq_maxee 1 (maximum expected errors 1), -fastq_truncqual 10 (truncating reads at first incidence of quality 10), -fastq_minlen 150 (minimum read length after other filtration steps), and -fastq_trunclen 150 (truncating reads at length 150 bp). Unique sequences were obtained by dereplicating using the VSEARCH v2.13.3[56] command --derep_fulllength, followed by removal of chimeric sequences using the VSEARCH command --uchime_denovo with default settings. The reads were mapped to a reference database containing the 16S rRNA gene sequences of the 34 experimental species with USEARCH -closed_ref command with > 97 % identity requirement. Problems associated with closed reference operational taxonomic unit (OTU) clustering for environmental bacterial communities[57], such as false positive genus assignment, should not apply to this case as the community is defined and has its own reference database. The two DNA extraction and amplicon sequencing batches (replicates 1–3 vs. replicates 4–8) display a minor but distinct batch effect in community composition (Figure 2). However, performing downstream analyses separately for the two batches did not affect the qualitative findings in the study.

For deep sequencing data, Cutadapt 1.12[53] was used to remove sequencing adapters and quality trim sequence data, with the parameters -O 10 (minimum overlap for an adapter match), -q 28 (quality

cutoff for the 3′ end of each read), and --minimum-length 30 (minimum length of trimmed read). Sequence data quality before and after Cutadapt was assessed using FastQC (www.bioinformatics.babraham.ac.uk/projects/fastqc) and MultiQC[54]. The deep sequencing data was mapped to a multi-FASTA file containing the whole-genome sequences of all experimental isolates (genome accessions indicated in [49]) except for one rare species lacking genome data (*Roseomonas gilardii* HAMBI 2470), using bowtie2[58] with default settings. The Picard command MarkDuplicates was used to mark duplicates in alignment (BAM) files after sorting with SAMtools[59]. Subsequently, BEDtools 2.2 was used to compute genome coverage in 1 kb windows[60]. This pan-genome mapping approach produced similar results compared to mapping the data to each genome individually, indicating that genome coverage was not reduced due to biased read recruitment in homologous regions, as well as cross-validating amplicon data (Extended Data Figure 8). Genome coverage data also indicated a lack of major copy number aberrations (Extended Data Figure 9).

Prior to variant calling and annotation, the metagenomic alignment files were split by species using SAMtools[59]. Alignment files containing below 200,000 reads, representing 5× genome coverage for a 4 Mb bacterial genome, were removed. Since differential genome coverage would affect variant count, nucleotide diversity and allele frequency estimates and thereby act as a confounder in downstream analyses comparing experimental treatments, all remaining BAM files were downsampled to 200,000 reads. Following this, genomic variants (SNPs and short INDELs) were called from BAM files with FreeBayes 1.1.0-60[61], using a population level approach (--pooled-continuous) and calling only one variant allele per locus (--use-best-n-alleles 1). Variants were filtered based on exceeding Phred-scaled quality 20 ("QUAL > 20") and read depth 2 ("DP > 2") using vcffilter from vcflib (https://github.com/vcflib/vcflib). This allowed detecting variants that had reached high frequency (min. 50 %) in a total of 229 samples representing abundant species in the experiment during (day

32) and after recovery from (day 48) the antibiotic pulse. Variants were annotated using SnpEff 4.3[62].

Ecological analyses

All analyses were performed in the R v3.6.1 environment[63]. The t-distributed stochastic neighbor embedding (t-SNE) map for Extended Data Figure 1 was created using the Rtsne package[64] with the options perplexity = 20 and theta = 0.5. Random forest models using community composition data to classify the antibiotic or immigration treatments after the antibiotic pulse or following the recovery period were generated using the randomForest package[65]. Before analyses, rare species were removed based on > 80 % of values being zero, and the data was standardized by converting each value into a Z-score (subtracting each sample's mean and dividing by the sample's standard deviation). Random forest classification was performed using the function randomForest implementing the Breiman's random forest algorithm, with the options importance = TRUE and proximities = TRUE. Subsequently, permutation tests (1,000 permutations) were implemented using the function rf.significance to test whether the models perform better than expected by chance. Following this, the function train in the package caret[66] was used to systematically partition the data into training and tests sets repeatedly using the leave-one-out cross-validation (LOOCV) approach to estimate model performance (accuracy).

The influence of the experimental treatments on KL divergence relative to the pre-disturbance state was investigated using generalized least squares models (gls) as implemented in the nlme package[67], specifying a residual variance structure dependent on the antibiotic level. The stepAIC function in the MASS package[68] was subsequently used to select the best model based on the Akaike information criterion (AIC). The competitive fitness of species during the antibiotic pulse or the recov-

500 ery period was estimated as the logarithm of the final frequency relative to the starting frequency,
501 which can be directly derived from the replicator equation in evolutionary game theory. The strain
502 *Azospirillum brasilense* HAMBI 3172 was chosen to be the reference and its logarithm of the final
503 frequency relative to the starting frequency was subtracted from all other values. To control for
504 noise from the frequency changes of low-abundance species and to award more weight to species
505 with high abundance in at least one of the estimated time points, a pseudocount constituting 1 %
506 proportion was added to the species abundance data prior to computing competitive fitness. The
507 effect of the experimental treatments on species extinction probability was tested using the base R
508 function glm with the option family = "binomial".
509
510 To quantify the repeatability of ecological dynamics, we used the diversity dissimilarity index[33]:
511

$$\frac{\frac{D_{pooled}}{D_{mean}} - 1}{M - 1}$$

512
513 where *D* is a diversity index (either Shannon diversity or species richness computed using the vegan
514 package[69]), and *M* is the number of communities whose species compositions are compared (over
515 time). If the species compositions of replicates are identical, the diversity of the pooled community
516 is equal to the mean diversity, and the diversity dissimilarity index equals 0, and if the communities
517 have no species in common, the index equals 1.
518
519 **Evolutionary analyses**
520
521 We used minimal criteria to filter raw genomic variants from the downsampled variant data prior to
522 downstream analyses. First, we removed data for one species, HAMBI 403, which had a large num-

523 ber of variants (130,000) indicative of an incorrect reference genome. Second, there were peaks
524 above 80 % in variant frequency distributions across the communities. Such a high level of parallel-
525 ism suggests that the variants are either ancestral or systematic sequencing errors, and variants oc-
526 curring in over 80 % of the communities were therefore removed.
527
528 From this variant data set, we extracted nonsynonymous mutations and devised a threshold for re-
529 currence. Of all the coding genes in all the genomes, we drew mutations from a multinomial distri-
530 bution with replacement. If these 588 mutations were randomly distributed over the 58,220 coding
531 genes in the genomes, we would expect only five genes mutated in two or more populations. In total,
532 there were 1092 coding nonsynonymous mutations across 47 genes independently mutated in two
533 or more populations. Therefore, we focused on multi-hit genes which were independently mutated
534 in two or more populations. This set was used for the statistical analysis below, while a larger set
535 from genomic variant data prior to downsampling, and also including the known streptomycin re-
536 sistance gene *rpsL*, was used for Figure 6 to present the maximum amount of functionally annotated
537 potential targets of selection.
538
539 We used permutational analysis of variance (PERMANOVA)[70] to test whether the antibiotic level
540 or presence/absence of immigration affected the targets of mutation. Each community was scored
541 by the presence (1) or absence (0) of a nonsynonymous mutation in each of the multi-hit genes, and
542 these data were used to calculate the Euclidian distance between populations[71]. Before performing
543 PERMANOVA, its assumption of homogeneity of multivariate dispersions within treatments was
544 tested with the betadisper function in the vegan package that uses the PERMDISP2 procedure as
545 described previously[72]. The adonis function in the vegan package was then used to test the probabil-
546 ity that the observed distances could arise by chance by comparing them with random permutations
547 of the raw data[73].

Data availability

Raw sequence data (fastq files) has been deposited in the NCBI Sequence Read Archive (SRA) under the accession PRJNA632457. All code and pre-processed data needed to reproduce the downstream analyses and figures are available via GitHub: https://github.com/johannescairns/repeatable_dynamics (permanent doi: https://doi.org/10.5281/zenodo.3908935).

References

1. Smith, M.D., Knapp, A.K. & Collins, S.L. A framework for assessing ecosystem dynamics in response to chronic resource alterations induced by global change. *Ecology* **90**, 3279–3289 (2009).
2. Rockstrom, J., et al. A safe operating space for humanity. *Nature* **461**, 472–475 (2009).
3. Morley, V.J., Woods, R.J. & Read, A.F. Bystander selection for antimicrobial resistance: Implications for patient health. *Trends Microbiol* **27**, 864–877 (2019).
4. Vrancken, G., Gregory, A.C., Huys, G.R.B., Faust, K. & Raes, J. Synthetic ecology of the human gut microbiota. *Nat Rev Microbiol* **17**, 754–763 (2019).
5. Lässig, M., Mustonen, V. & Walczak, A.M. Predicting evolution. *Nat Ecol Evol* **1**, 77 (2017).
6. Robinson, J.I., et al. Metabolomic networks connect host-microbiome processes to human *Clostridioides difficile* infections. *J Clin Invest* **130**, 3792–3806 (2019).
7. Oh, S., Choi, D. & Cha, C.J. Ecological processes underpinning microbial community structure during exposure to subinhibitory level of triclosan. *Sci Rep* **9**, 4598 (2019).

8. Zorner, P., Farmer, S. & Alibek, K. Quantifying crop rhizosphere microbiome ecology: The next frontier in enhancing the commercial utility of agricultural microbes. *Ind Biotechnol (New Rochelle N Y)* **14**, 116–119 (2018).
9. Lozada-Gobilard, S., et al. Environmental filtering predicts plant-community trait distribution and diversity: Kettle holes as models of meta-community systems. *Ecol Evol* **9**, 1898–1910 (2019).
10. Li, J., et al. Shared molecular targets confer resistance over short and long evolutionary time-scales. *Mol Biol Evol* **36**, 691–708 (2019).
11. Vázquez-García, I., et al. Clonal heterogeneity influences the fate of new adaptive mutations. *Cell Rep* **21**, 732–744 (2017).
12. Illingworth, C.J.R., Parts, L., Schiffels, S., Liti, G. & Mustonen, V. Quantifying selection acting on a complex trait using allele frequency time series data. *Mol Biol Evol* **29**, 1187–1197 (2012).
13. Leibler, S. & Kussell, E. Individual histories and selection in heterogeneous populations. *Proc Natl Acad Sci U S A* **107**, 13183–13188 (2010).
14. Des Roches, S., et al. The ecological importance of intraspecific variation. *Nat Ecol Evol* **2**, 57–64 (2018).
15. Wistrand-Yuen, E., et al. Evolution of high-level resistance during low-level antibiotic exposure. *Nat Commun* **9**, 1599 (2018).
16. Schoener, T.W. The newest synthesis: Understanding the interplay of evolutionary and ecological dynamics. *Science* **331**, 426–429 (2011).
17. Scheuerl, T., et al. Bacterial adaptation is constrained in complex communities. *Nat Commun* **11**, 754 (2020).

18. Roodgar, M., et al. Longitudinal linked read sequencing reveals ecological and evolutionary responses of a human gut microbiome during antibiotic treatment. *bioRxiv* 2019.12.21.886093. doi:https://doi.org/10.1101/2019.12.21.886093
19. Dethlefsen, L. & Relman, D.A. Incomplete recovery and individualized responses of the human distal gut microbiota to repeated antibiotic perturbation. *Proc Natl Acad Sci U S A* **108**, S1:4554–4561 (2011).
20. Palleja, A., et al. Recovery of gut microbiota of healthy adults following antibiotic exposure. *Nat Microbiol* **3**, 1255–1265 (2018).
21. Jernberg, C., Lofmark, S., Edlund, C. & Jansson, J.K. Long-term ecological impacts of antibiotic administration on the human intestinal microbiota. *ISME J* **1**, 56–66 (2007).
22. Yassour, M., et al. Natural history of the infant gut microbiome and impact of antibiotic treatment on bacterial strain diversity and stability. *Sci Transl Med* **8**, 343ra81 (2016).
23. Mack, I., et al. Antimicrobial resistance following azithromycin mass drug administration: Potential surveillance strategies to assess public health impact. *Clin Infect Dis* **pii**, ciz893 (2019).
24. Tamburini, S., Shen, N., Wu, H.C. & Clemente, J.C. The microbiome in early life: Implications for health outcomes. *Nat Med* **22**, 713–722 (2016).
25. Langdon, A., Crook, N. & Dantas, G. The effects of antibiotics on the microbiome throughout development and alternative approaches for therapeutic modulation. *Genome Med* **8**, 39 (2016).
26. Brown, J.H. & Kodricbrown, A. Turnover rates in insular biogeography: Effect of immigration on extinction. *Ecology* **58**, 445–449 (1977).
27. Patel, R. & DuPont, H.L. New approaches for bacteriotherapy: Prebiotics, new-generation probiotics, and synbiotics. *Clin Infect Dis* **60**, S2:108–121 (2015).
28. Lawley, T.D., et al. Targeted restoration of the intestinal microbiota with a simple, defined bacteriotherapy resolves relapsing *Clostridium difficile* disease in mice. *PLoS Pathog* **8**, e1002995 (2012).

29. Ingrisch, J. & Bahn, M. Towards a comparable quantification of resilience. *Trends Ecol Evol* **33**, 251–259 (2018).
30. Morton, J.T., et al. Establishing microbial composition measurement standards with reference frames. *Nat Commun* **10**, 2719 (2019).
31. Trindade, S., Sousa, A. & Gordo, I. Antibiotic resistance and stress in the light of Fisher's model. *Evolution* **66**, 3815–3824 (2012).
32. Day, T., Huijben, V. & Read, A.F. Is selection relevant in the evolutionary emergence of drug resistance? *Trends Microbiol* **23**, 126–133 (2015).
33. Lerner, J., et al. Chromosomal barcoding of *E. coli* populations reveals lineage diversity dynamics at high resolution. *bioRxiv* 571505. doi:https://doi.org/10.1101/571505
34. Springer, B., et al. Mechanisms of streptomycin resistance: Selection of mutations in the 16S rRNA gene conferring resistance. *Antimicrob Agents Chemother* **45**, 2877–2884 (2001).
35. Nishimura, K., Hosaka, T., Tokuyama, S., Okamoto, S. & Ochi, K. Mutations in *rsmG*, encoding a 16S rRNA methyltransferase, result in low-level streptomycin resistance and antibiotic overproduction in *Streptomyces coelicolor* A3(2). *J Bacteriol* **189**, 3876–3883 (2007).
36. Macfarlane, E.L.A., Kwasnicka, A. & Hancock, R.E.W. Role of *Pseudomonas aeruginosa* PhoP-phoQ in resistance to antimicrobial cationic peptides and aminoglycosides. *Microbiology* **146**, Pt 10:2543–2554 (2000).
37. Girgis, H.S., Hottes, A.K. & Tavazoie, S. Genetic architecture of intrinsic antibiotic susceptibility. *PLOS ONE* **4**, e5629 (2009).
38. Yongjuan Liu, X.C., Long Pan & Zhonggui Mao. Differential protein expression of a streptomycin-resistant *Streptomyces albulus* mutant in high yield production of ε-poly-l-lysine: A proteomics study. *RSC Adv* **9**, 24092 (2019).
39. Beardmore, R.E., et al. Drug-mediated metabolic tipping between antibiotic resistant states in a mixed-species community. *Nat Ecol Evol* **2**, 1312–1320 (2018).

40. Perron, G.G., Gonzalez, A. & Buckling, A. The rate of environmental change drives adaptation to an antibiotic sink. *J Evol Biol* **21**, 1724–1731 (2008).
41. Retel, C., et al. The feedback between selection and demography shapes genomic diversity during coevolution. *Sci Adv* **5**, eaax0530 (2019).
42. Melnyk, A.H., Wong, A. & Kassen, R. The fitness costs of antibiotic resistance mutations. *Evol Appl* **8**, 273–283 (2015).
43. Wein, T., et al. Carrying capacity and colonization dynamics of *Curvibacter* in the *Hydra* host habitat. *Front Microbiol* **9**, 443 (2018).
44. Zhou, J., et al. Stochastic assembly leads to alternative communities with distinct functions in a bioreactor microbial community. *mBio* **4**, e00584-12 (2013).
45. Lozupone, C.A., Stombaugh, J.I., Gordon, J.I., Jansson, J.K. & Knight, R. Diversity, stability and resilience of the human gut microbiota. *Nature* **489**, 220–230 (2012).
46. Shade, A., et al. Fundamentals of microbial community resistance and resilience. *Front Microbiol* **3**, 417 (2012).
47. Waples, R.S., Beechie, T. & Pess, G.R. Evolutionary history, habitat disturbance regimes, and anthropogenic changes: What do these mean for resilience of Pacific salmon populations? *Ecol Soc* **14**, 3 (2009).
48. Johnstone, J.F., et al. Changing disturbance regimes, ecological memory, and forest resilience. *Front Ecol Environ* **14**, 369–378 (2016).
49. Cairns, J., et al. Construction and characterization of synthetic bacterial community for experimental ecology and evolution. *Front Genet* **9**, 312 (2018).
50. Datta, N., Hedges, R.W., Shaw, E.J., Sykes, R.B. & Richmond, M.H. Properties of an R factor from *Pseudomonas aeruginosa*. *J Bacteriol* **108**, 1244–1249 (1971).
51. Cairns, J., et al. Ecology determines how low antibiotic concentration impacts community composition and horizontal transfer of resistance genes. *Commun Biol* **1**, 35 (2018).

52. Zhang, J., Kobert, K., Flouri, T. & Stamatakis, A. PEAR: A fast and accurate Illumina Paired-End reAd mergeR. *Bioinformatics* **30**, 614–620 (2014).
53. Martin, M. & Martin, M. Cutadapt removes adapter sequences from high-throughput sequencing reads. *Embnet.journal* **17**, 10–12 (2011).
54. Ewels, P., Magnusson, M., Lundin, S. & Kaller, M. MultiQC: Summarize analysis results for multiple tools and samples in a single report. *Bioinformatics* **32**, 3047–3048 (2016).
55. Edgar, R.C. UPARSE: Highly accurate OTU sequences from microbial amplicon reads. *Nat Methods* **10**, 996–998 (2013).
56. Rognes, T., Flouri, T., Nichols, B., Quince, C. & Mahe, F. VSEARCH: A versatile open source tool for metagenomics. *PeerJ* **4**, e2584 (2016).
57. Edgar, R.C. Accuracy of microbial community diversity estimated by closed- and open-reference OTUs. *PeerJ* **5**, e3889 (2017).
58. Langmead, B. & Salzberg, S.L. Fast gapped-read alignment with Bowtie 2. *Nat Methods* **9**, 357–359 (2012).
59. Li, H., et al. The Sequence Alignment/Map format and SAMtools. *Bioinformatics* **25**, 2078–2079 (2009).
60. Quinlan, A.R. & Hall, I.M. BEDTools: A flexible suite of utilities for comparing genomic features. *Bioinformatics* **26**, 841–842 (2010).
61. Garrison, E. & Gabor, M. Haplotype-based variant detection from short-read sequencing. *arXiv* 1207.3907 (2012).
62. Cingolani, P., et al. A program for annotating and predicting the effects of single nucleotide polymorphisms, SnpEff: SNPs in the genome of *Drosophila melanogaster* strain w(1118); iso-2; iso-3. *Fly* **6**, 80–92 (2012).
63. R Core Team. R: A language and environment for statistical computing. R Foundation for Statistical Computing, Vienna, Austria (2019). URL:https://www.R-project.org/.

64. Krijthe, J. Rtsne: T-distributed stochastic neighbor embedding using a Barnes-Hut implementation. R package version 0.15 (2015). URL:https://github.com/jkrijthe/Rtsne
65. Liaw, A. & Wiener, M. Classification and regression by randomForest. *R News* **2**, 18–22 (2002).
66. Kuhn, M., et al. caret: Classification and regression training. R package version 6.0-84 (2019). URL:https://CRAN.R-project.org/package=caret
67. Pinheiro, J, Bates, D., DebRoy, S., Sarkar, D. & R Core Team. nlme: Linear and nonlinear mixed effects models. R package version 3.1-142 (2019). URL:https://CRAN.R-project.org/package=nlme
68. Venables, W.N. & Ripley, B.D. Modern applied statistics with S. Fourth Edition, Springer, New York (2002).
69. Oksanen, J, et al. vegan: Community ecology package. R package version 2.5-6 (2019). URL:https://CRAN.R-project.org/package=vegan
70. Zapala, M.A. & Schork, N.J. Multivariate regression analysis of distance matrices for testing associations between gene expression patterns and related variables. *Proc Natl Acad Sci U S A* **103**, 19430–19435 (2006).
71. Excoffier, L., Smouse, P.E. & Quattro, J.M. Analysis of molecular variance inferred from metric distances among DNA haplotypes: Application to human mitochondrial DNA restriction data. *Genetics* **131**, 479–491 (1992).
72. Anderson, M.J. Distance-based tests for homogeneity of multivariate dispersions. *Biometrics* **62**, 245–253 (2006).
73. Anderson, M.J. A new method for non-parametric multivariate analysis of variance. *Austral Ecol* **26**, 32–46 (2001).

Acknowledgements

We thank Aki Ronkainen and Paula Typpö for technical assistance. This work was funded by the Academy of Finland (grant 106993 to TH; grant 313270 to VM), Jenny and Antti Wihuri Foundation (grant 190040 to JC), and the Heisenberg Stipend from the German Research Foundation (DFG; grant 4135/9 to LB).

Author contributions

Design of serial passage experiment: TH, JC, LB. Performing serial passage experiment: RJ. Design of data analysis: JC, VM, LB. Performing data analysis: JC. Interpreting results: JC, TH, LB, VM. JC wrote the first manuscript draft, with contributions from all authors. All authors approve the final version of the manuscript.

Competing interests

The authors state that they have no competing interests.

Figure legends

Figure 1. Experimental design. (A) Physical setup. A serial passage experiment was conducted with a 34-species artificial community in deep 96-well plates. Initial key traits of community members (intrinsic growth rate, represented by growth curve with yellow background, and intrinsic antibiotic susceptibility level, represented by growth curve in purple background) were measured separately for individual isolates used to construct the community. (B) Layout of antibiotic pulse experiment. The experiment consisted of serial propagation at 4-day (96 h) intervals for three 16-day epochs: an acclimation period, an antibiotic pulse period with three different levels of pulse antibiotic disturbance together with an antibiotic-free control treatment, and a recovery period. To investigate the role of species immigration, the full experiment was performed without and with reintroducing a small amount (1:500 cells relative to serial transfer inoculum) of the original community at each transfer. Each unique treatment combination was replicated eight times. Samples (N = 192) were collected for DNA extraction prior to the pulse (T0), after the pulse (T1) and after recovery (T2) to track community composition (amplicon sequencing) and genomic evolution (metagenomic sequencing).

Figure 2. Community dynamics during antibiotic pulse experiment. The figure depicts the frequencies of abundant species across time in eight replicate communities for each unique treatment combination indicated on the right (low, intermediate and high antibiotic levels correspond to 4, 16 and 128 μg ml^{-1} streptomycin, respectively). The shaded area shows the antibiotic pulse epoch, with increasingly dark hue indicating increasing antibiotic level. The top four panels show the different antibiotic levels for the immigration-free treatment and the bottom four panels for the immigration treatment. The *y*-axis has been square root transformed and scaled 0–1 to allow visual discernment of less abundant species. "Others" denotes rare taxa that fail to reach a frequency of 5 % in at least one community and time point. In total, 190 experimental samples are included in the figure together with one stock community sample to represent initial species composition for all communities. For two communities, adequate amplicon sequence data could not be recovered for day 48.

Figure 3. Community response to antibiotic perturbation. (A) Shannon diversity at the end of the antibiotic pulse (N = 64). (B) Ecological resilience without (left) and with (right) species immigration (N = 190). Resilience has been quantified for each community separately as the Kullback-Leibler (KL) divergence of community composition over time after the disturbance relative to the pre-disturbance state. In both panels, the data for the respective metric (Shannon diversity or KL divergence, both computed from species composition data) is displayed by a box and whiskers plot overlaid by raw data points. The lower and upper hinges of the box and whiskers plot correspond to the 25^{th} and 75^{th} percentiles, while the lower and upper and whiskers extend from the hinge to the smallest or largest value, respectively (max. 1.5 × interquartile range from hinge). Low, intermediate and high antibiotic levels correspond to 4, 16 and 128 μg ml^{-1} streptomycin, respectively.

Figure 4. Competitive fitness of species in replicate communities (N = 8) during and after recovery from intermediate-level antibiotic pulse (16 μg ml^{-1} streptomycin) in the absence of immigration (mean indicated by dashed line). The figure illustrates the repeatability of the species response between replicate communities and the inverse response for multiple species during the perturbation (top panel) versus recovery (bottom panel) phases. The competitive fitness of species is estimated

as the logarithm of the final frequency relative to the starting frequency, derived from the replicator equation in evolutionary game theory. Data for replicate 7 is missing from the panel below because of inadequate amplicon sequence data for one community sample (final time point).

Figure 5. Repeatability of community trajectories, assessed using the diversity dissimilarity index (± bootstrapped standard error; N = 190) where zero indicates perfect identity and one complete dissimilarity between replicate communities. Repeatability is shown separately for Shannon diversity (top), which gives more weight to abundant species, and species richness (bottom), which gives equal weight to all species. The antibiotic pulse epoch is indicated by grey shade. Low, intermediate and high antibiotic levels correspond to 4, 16 and 128 μg ml^{-1} streptomycin, respectively. The diversity dissimilarity index has been computed from species compositional data.

Figure 6. Targets of adaptive mutations reaching high frequencies (> 0.3 to fixation) in high-abundance species during or after recovery from antibiotic pulse. The same mutations were mostly observed in both time points when the species was detectable (i.e. mutation not lost during recovery). The heat map shows functionally annotated targets of recurrent nonsynonymous mutations, as well as the known streptomycin resistance gene *rpsL* which is only mutated in a single community. Since the genomic variants were recovered from deep sequencing data, they could only be confirmed for a subset of the three sequenced replicates and experimental treatments owing to differential abundance of species and volume of sequence data. Color coding is used to indicate the number of the replicates where a genomic target of interest was mutated relative to the number for which genomic variant data could be recovered in a particular experimental treatment.

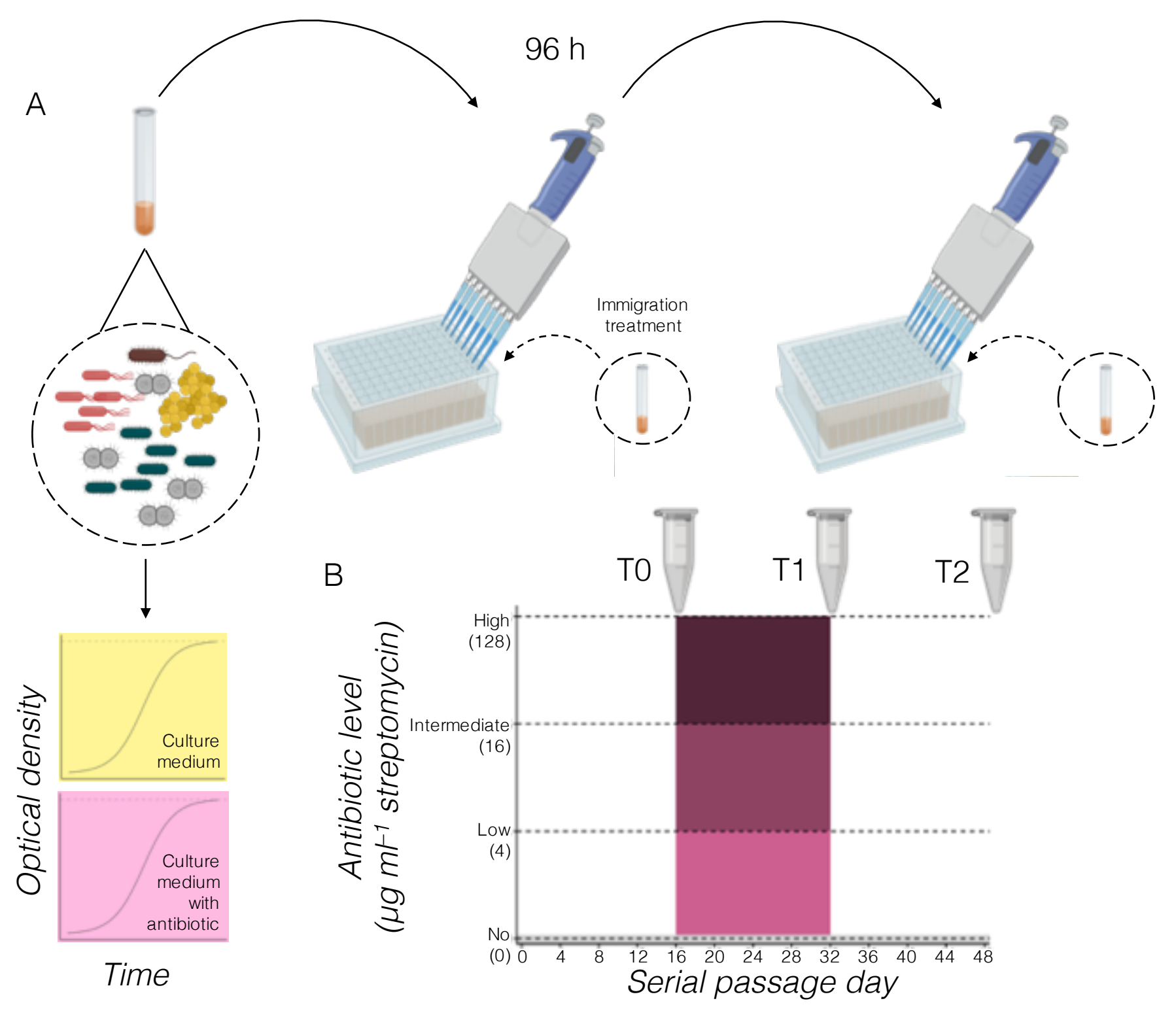
A
96 h
Immigration
treatment
Optical density
Culture
medium
Culture
medium
with
antibiotic
Time
B
T0
T1
T2
Antibiotic level
(μg ml⁻¹ streptomycin)
High
(128)
Intermediate
(16)
Low
(4)
No
(0)
0
4
8
12
16
20
24
28
32
36
40
44
48
Serial passage day

1 2 3 4 5 6 7 8

No immigration — No antibiotic
No immigration — Low antibiotic
No immigration — Intermediate antibiotic
No immigration — High antibiotic
Immigration — No antibiotic
Immigration — Low antibiotic
Immigration — Intermediate antibiotic
Immigration — High antibiotic

Species abundance (sqrt transformed and rescaled 0–1)

0.0 0.2 0.4 0.6 0.8 1.0

0 16 32 48

Day

- *Elizabethkingia meningoseptica HAMBI 1875*
- *Citrobacter koseri HAMBI 1287*
- *Aeromonas caviae HAMBI 1972*
- *Pseudomonas chlororaphis HAMBI 1977*
- *Sphingobacterium spiritivorum HAMBI 1896*
- *Sphingobacterium multivorum HAMBI 1874*
- *Agrobacterium tumefaciens HAMBI 105*
- *Morganella morganii HAMBI 1292*
- *Myroides odoratus HAMBI 1923*
- *Bordetella avium HAMBI 2160*
- *Niabella yanshanensis HAMBI 3031*
- *Azospirillum brasilense HAMBI 3172*
- *Stenotrophomonas maltophilia HAMBI 2659*
- *Paracoccus denitrificans HAMBI 2443*
- *Comamonas testosteroni HAMBI 403*
- *Sphingobium yanoikuyae HAMBI 1842*
- *Azorhizobium caulinodans HAMBI 216*
- *Hafnia alvei HAMBI 1279*
- *Others*

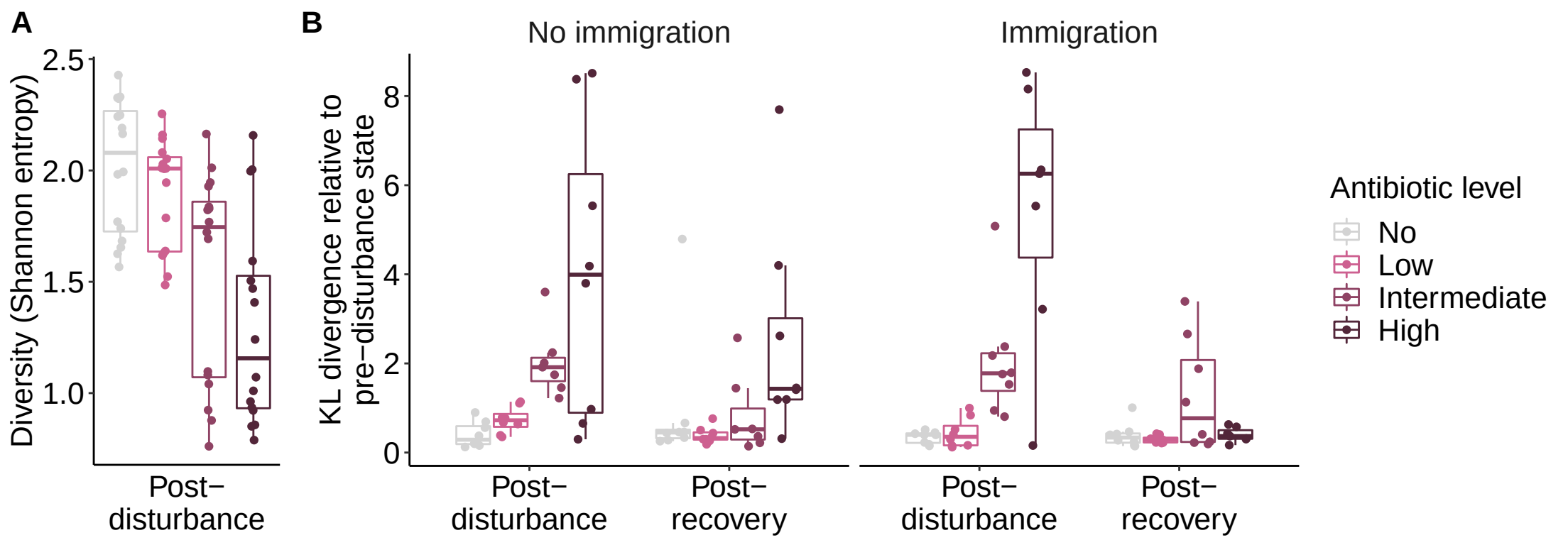
A
B
Diversity (Shannon entropy)
2.5
2.0
1.5
1.0
Post−
disturbance
KL divergence relative to
pre−disturbance state
No immigration
Immigration
8
6
4
2
0
Post−
disturbance
Post−
recovery
Post−
disturbance
Post−
recovery
Antibiotic level
No
Low
Intermediate
High

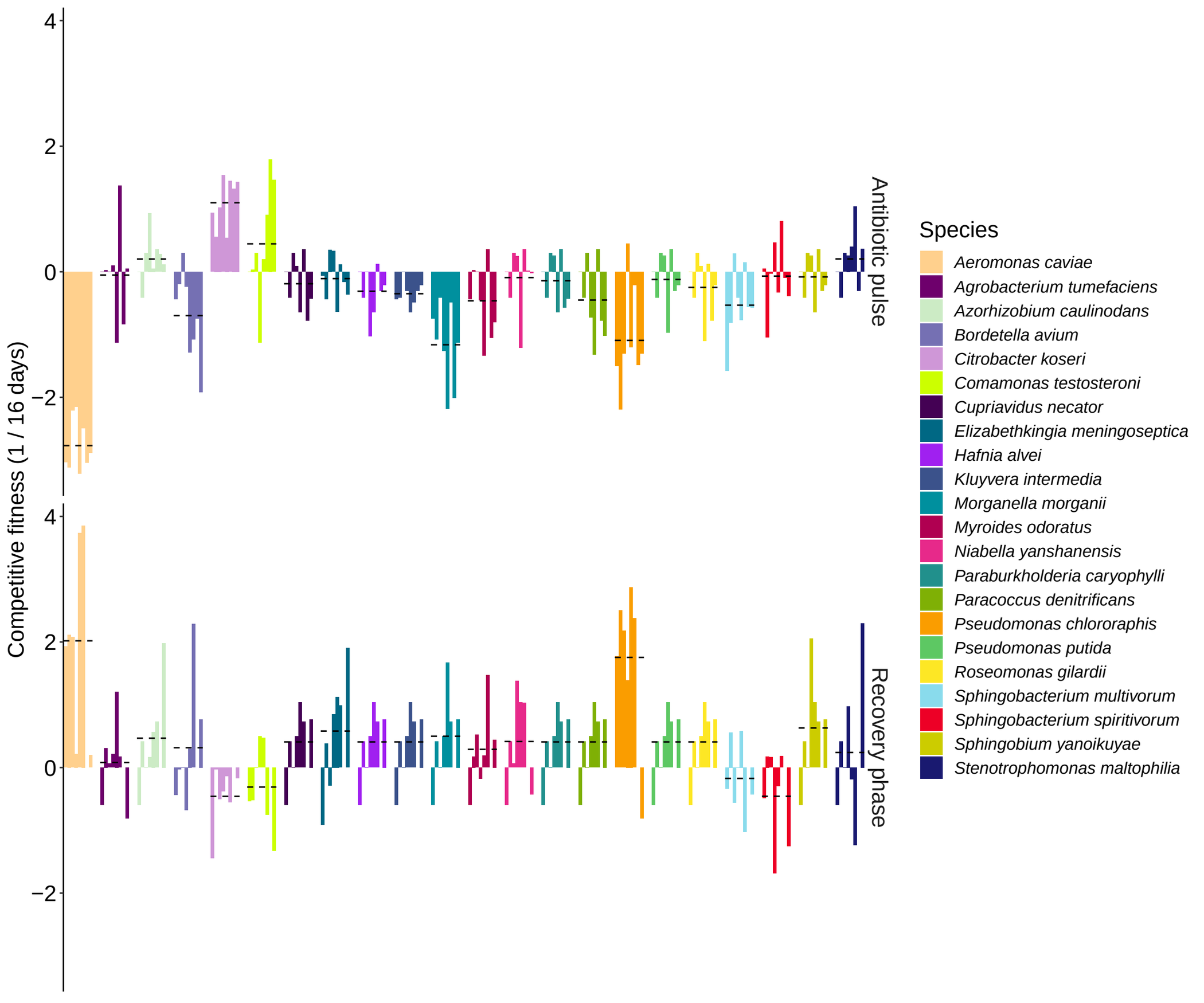
Competitive fitness (1 / 16 days)
4
2
0
−2
Antibiotic pulse
Recovery phase
Species
Aeromonas caviae
Agrobacterium tumefaciens
Azorhizobium caulinodans
Bordetella avium
Citrobacter koseri
Comamonas testosteroni
Cupriavidus necator
Elizabethkingia meningoseptica
Hafnia alvei
Kluyvera intermedia
Morganella morganii
Myroides odoratus
Niabella yanshanensis
Paraburkholderia caryophylli
Paracoccus denitrificans
Pseudomonas chlororaphis
Pseudomonas putida
Roseomonas gilardii
Sphingobacterium multivorum
Sphingobacterium spiritivorum
Sphingobium yanoikuyae
Stenotrophomonas maltophilia

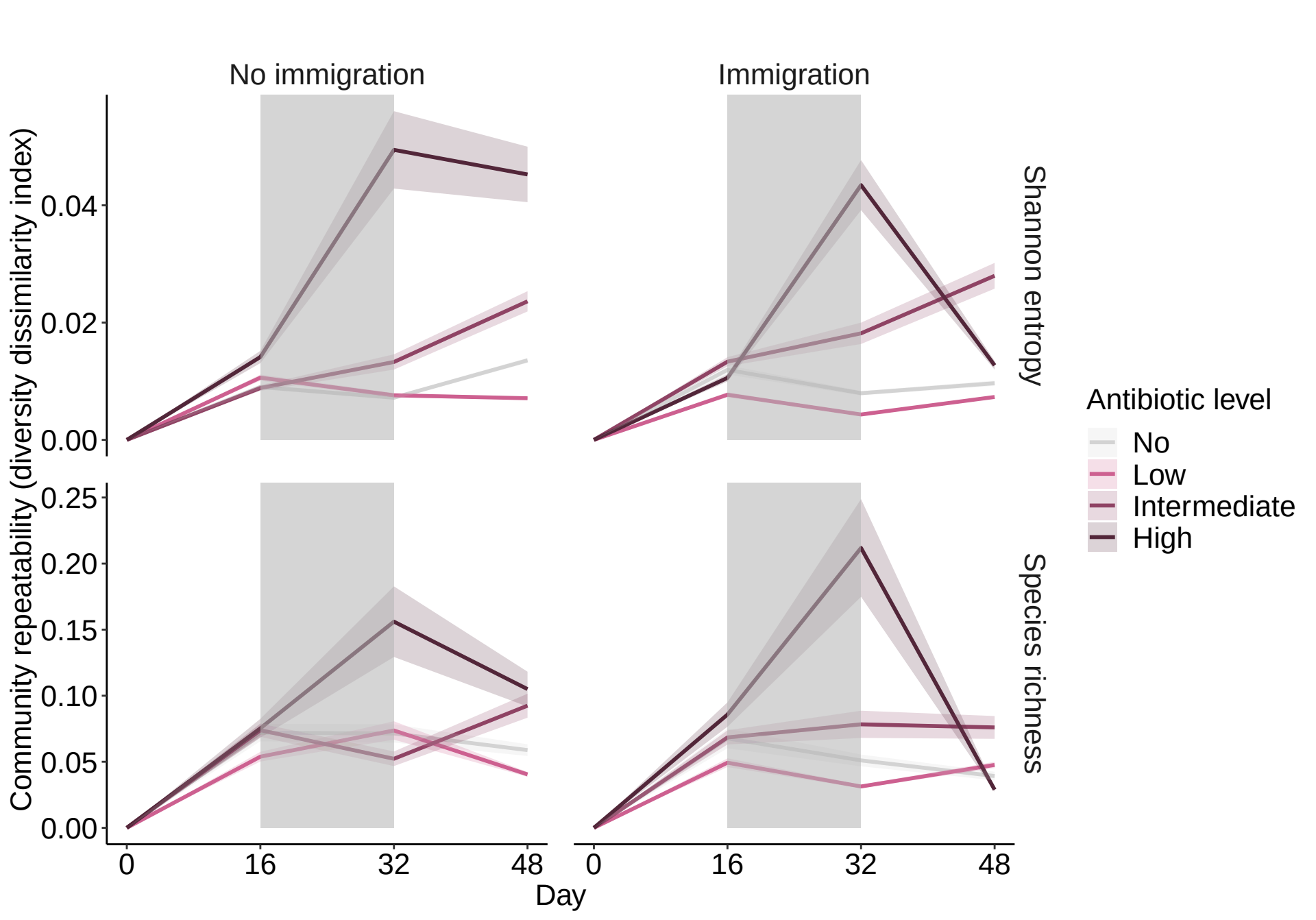
No immigration
Immigration
Shannon entropy
Species richness
Community repeatability (diversity dissimilarity index)
0.00
0.02
0.04
0.05
0.10
0.15
0.20
0.25
0
16
32
48
Day
Antibiotic level
No
Low
Intermediate
High

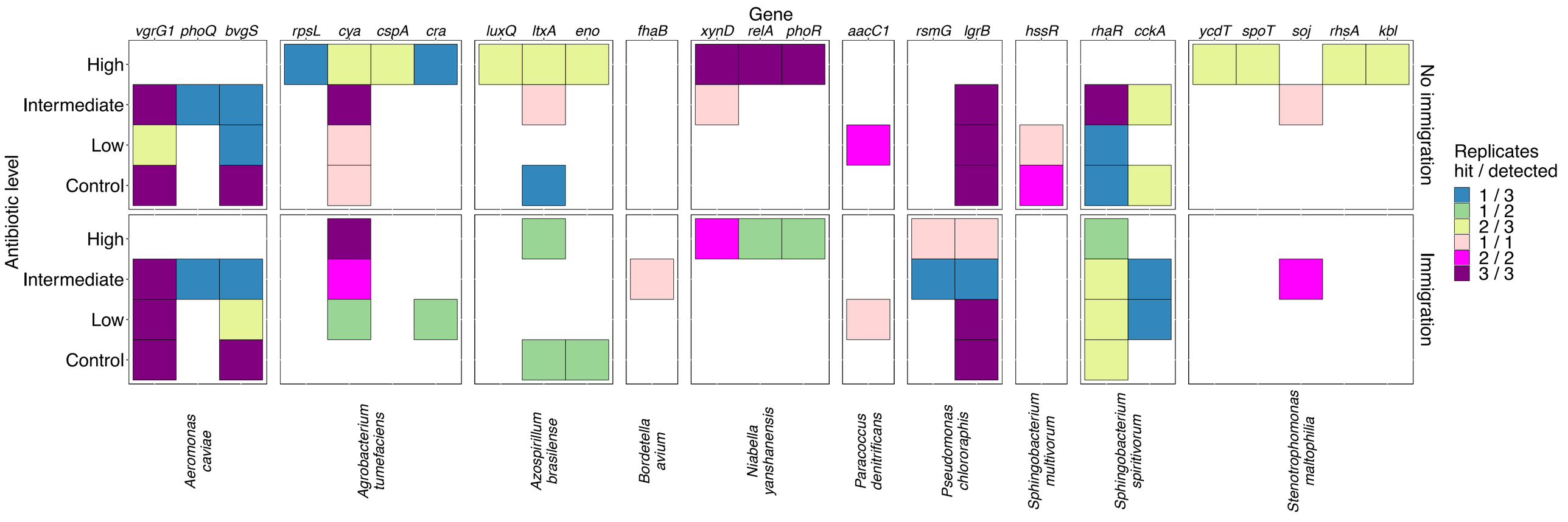
Gene
vgrG1 phoQ bvgS
rpsL cya cspA cra
luxQ ltxA eno
fhaB
xynD relA phoR
aacC1
rsmG lgrB
hssR
rhaR cckA
ycdT spoT soj rhsA kbl
Antibiotic level
High
Intermediate
Low
Control
No immigration
Immigration
Replicates hit / detected
1 / 3
1 / 2
2 / 3
1 / 1
2 / 2
3 / 3
Aeromonas caviae
Agrobacterium tumefaciens
Azospirillum brasilense
Bordetella avium
Niabella yanshanensis
Paracoccus denitrificans
Pseudomonas chlororaphis
Sphingobacterium multivorum
Sphingobacterium spiritivorum
Stenotrophomonas maltophilia